Commercial microwave link networks for rainfall observation: assessment of the current status and future challenges

Christian Chwala, Harald Kunstmann

Angaben zur Veröffentlichung / Publication details:

Chwala, Christian, and Harald Kunstmann. 2019. "Commercial microwave link networks for rainfall observation: assessment of the current status and future challenges." *Wiley Interdisciplinary Reviews: Water* 6 (2): e1337. https://doi.org/10.1002/wat2.1337.

Received: 15 March 2018 | Revised: 23 December 2018 | Accepted: 30 December 2018

DOI: 10.1002/wat2.1337

WILEY WIREs WATER

ADVANCED REVIEW

Commercial microwave link networks for rainfall observation: Assessment of the current status and future challenges

Christian Chwala[1] | Harald Kunstmann[1,2]

[1]Institute of Meteorology and Climate Research (IMK-IFU), Karlsruhe Institute of Technology, Garmisch-Partenkirchen, Germany

[2]Chair for Regional Climate and Hydrology, University of Augsburg, Augsburg, Germany

Correspondence
Christian Chwala, Institute of Meteorology and Climate Research (IMK-IFU), Karlsruhe Institute of Technology, Garmisch-Partenkirchen, Germany
Email: christian.chwala@kit.edu

Funding information
German Research Foundation

Accurate observation of the high spatio-temporal variability of rainfall is crucial for hydrometeorological applications. However, the existing observations from rain gauges and weather radars have individual shortcomings that can introduce considerable errors and uncertainties. A fairly new technique to get additional rainfall information is the usage of the country-wide commercial microwave link (CML) networks for rainfall estimation by exploiting the measurements of rain-induced attenuation along these CMLs. This technique has seen an increasing number of applications during the last years. Different methods have been developed to process the noisy raw data and to derive rainfall fields. It has been shown that CMLs can provide important line-integrated rainfall information that complements pointwise rain gauge and spatial radar observations. There exist several limitations, though. Robustly dealing with the erratic fluctuations of the CML raw data is a challenge, in particular with the growing number of CMLs. How to correctly compensate for the biases from the effect of wet antenna attenuation for different CMLs also remains a crucial research question. Progress is additionally hampered by the lack of method intercomparisons, which in turn is hampered by restricted data sharing. Hence, collaboration is key for further advancements, also with regard to extended interaction with the CML network operators, which is a prerequisite to achieve increased data availability. In regions where rain gauges and weather radars are available, CMLs are a welcome complement. But in developing countries, which are characterized by weak technical infrastructure and which often suffer from water stress, additional rainfall information is a necessity. CMLs could play a crucial role in this respect.

This article is categorized under:
Science of Water > Hydrological Processes
Science of Water > Water Quality
Science of Water > Methods

KEYWORDS
microwave link, precipitation, radar, rainfall, remote sensing

1 | INTRODUCTION

1.1 | Motivation

Observing and understanding the hydrological cycle is crucial to mitigate current and future water-related problems. Improved water management is required in many water-sensitive regions where continuing population growth will further increase water

stress (Vörösmarty, Green, Salisbury, & Lammers, 2000). In addition, potentially more frequent flooding events, due to regional increase of rainfall variability with more extreme events (Berg, Moseley, & Haerter, 2013) induced by increasing temperature levels, will require improved methods for flood nowcasting and forecasting.

Since precipitation is the main driver of the terrestrial part of the hydrological cycle, its accurate observation is therefore key for these required improvements. However, due to its high spatio-temporal variability, precipitation observation is still a scientific challenge.

Classical rain gauge networks suffer from the fact that rain gauge measurements, being point observations, only have a low spatial representativeness. In addition, wind and exposure-induced errors increase uncertainties (Nešpor & Sevruk, 1999). In contrast to the point observations of rain gauges, weather radars provide rainfall information over large areas (several tens of square kilometers). However, the relation of measured reflectivity Z and rain rate R has a strong dependence on the usually unknown drop size distribution (Ulbrich & Lee, 1999). Further uncertainties stem from the variability of the vertical profile of reflectivity (Hazenberg, Leijnse, & Uijlenhoet, 2011), ground clutter, (partial) beam blockage and bright band interception (Andrieu, Creutin, Delrieu, & Faure, 1997). Advancement of weather radar technology, namely the exploitation of dual-polarization measurements, has allowed the community to mainly overcome the limitations of the Z-R relation, ground clutter and hail contamination. Beam blockage and the vertical profile of reflectivity however still remain a limiting factor (Berne & Krajewski, 2013). A major drawback of both radar and rain gauges, is the limited availability in many parts of the world. This is why precipitation observation on a continental or global scale requires measurements from spaceborne sensors. With the launch of the core satellite of the global precipitation measurement mission (GPM) this research field recently accomplished significant progress (Hou et al., 2013). For small spatial- and temporal scales, for example, for hydrological modeling in urban or mountainous catchments, the provided resolution is, however, often still too coarse. Uncertainties in the absolute values of the provided precipitation estimates (Rios Gaona et al., 2017) also limit their applicability for hydrometeorological applications.

The fairly new technique of rainfall estimation from large commercial microwave link (CML) networks, operated as backhaul of the cell phone network, is a possible solution for improving rainfall observations. CMLs can provide missing near ground rainfall observations in sparsely gauged regions, they can complement existing observations in regions covered by conventional monitoring networks and they can improve the space–time resolution and accuracy of rainfall products.

1.2 | Outline

In this advanced review paper we given an introduction to the technique of rainfall estimation with CML networks, provide an overview of the current achievements and critically assess the limitations and future challenges of this technique.

Later in this introductory Section 1 we give a brief explanation of the principles of the technique and provide a short retrospect of the developments that led to its discovery. In Section 2, we present the typical processing steps required to derive rainfall information from CML data and elaborate on their individual challenges. The following Section 3 summarizes and assesses the state of art, based on which we identify crucial limitations and discuss future challenges of rainfall estimation from CML data in Section 4.

Compared to the primer provided by Uijlenhoet, Overeem, and Leijnse (2018) which provides an introduction and overview of this topic, aimed to be understood by a very general audience, we emphasize on discussing and assessing the related challenges. In particular, we focus on the issues of erratic CML signal fluctuations and wet antenna attenuation. In the

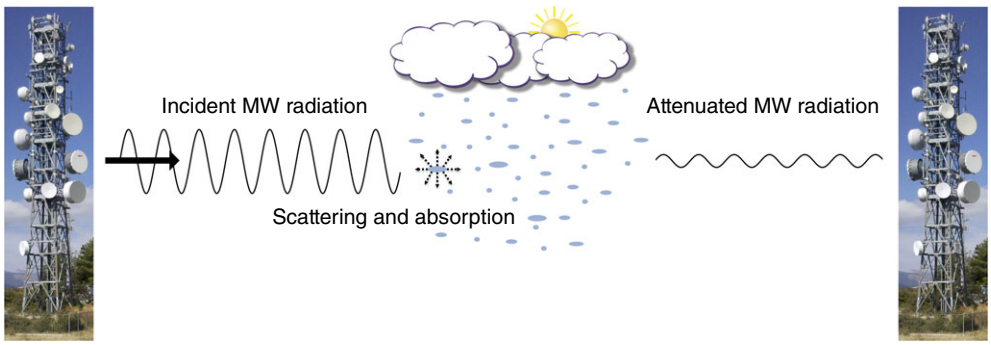

FIGURE 1 Illustration of the basic operating principle of CML rainfall estimation. CMLs (with the drum-shaped antennas) are typically used to interconnect cell phone towers. Due to scattering and absorption the transmitted microwave (MW) radiation is attenuated by raindrops. This leads to an attenuated signal level at the receiver, from which the rain rate along the path can be estimated

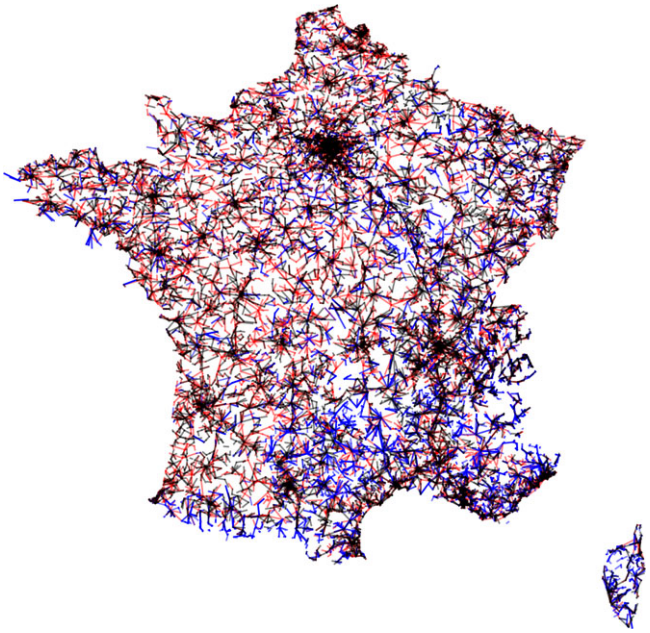

FIGURE 2 CML network of the three largest cell phone providers in France. Data of CML transmitter and receiver location and orientation is provided by the French National Frequencies Agency (ANFR). From this data, CML paths were derived and made available[3]

discussion section we also spell out our view on the future challenges of this technique and suggest possible approaches to tackle them.

1.3 | Principle of CML rainfall estimation

A CML provides a line of sight radio connection between two locations. They are commonly used to interconnect cell phone base station towers as shown in Figure 1, but are also employed by other operators, for example, by skiing resorts to connect their summit stations. Current CMLs typically use frequencies between 5 GHz and 40 GHz. With the recently started installation of E-band CMLs, the common frequency range will be extended to 80 GHz. The technique of rainfall estimation using CMLs is based on the fact that rainfall considerably attenuates electromagnetic radiation at these frequencies, in particular above 15 GHz. A measurement of rain-induced attenuation can be used to derive the average rain rate along the path. Combined with the large number of available CMLs, for example, shown for France in Figure 2, CML networks can provide county-wide rainfall observations.

The relation between rain induced attenuation k in dB/km and the rain rate R in mm/hr can be described with the simple power law

$$k = a\,R^b, \tag{1}$$

where a and b depend on the microwave radiation's frequency and polarization, the rain drop temperature and to a much lesser extent, on the rain drop size distribution (DSD). Compared to the weather radar Z-R relation between radar reflectivity and rain rate, which can be expressed as a similar power law, the k-R relation is far less sensitive to variation of the DSD. As can be seen in Figure 3 the scatter of k and R calculated from DSD observations is very low compared to the scatter of Z versus R, in particular for k-R at 20 GHz. The value of a, given for the k-R fit for each frequency, increases with increasing frequency. That is, high frequencies experience stronger attenuation for the same amount of rain. The value of b is close to 1, in particular around 30 GHz, making Equation 1 linear, or almost linear.

The linearity of Equation 1 is an important property of the k-R relation, since the measured attenuation is the path integrated attenuation A in dB which is related to the path averaged rain rate $\bar{R}$ in mm/hr via

$$A = \int_0^L k(l)dl = \int_0^L a\,R(l)^b\,dl \overset{b\approx 1}{=} a\,\bar{R}^b\,L, \tag{2}$$

where L is the length of the path between transmitter and receiver in km. Thus, the further b deviates from 1, the larger the biases are that are introduced by heterogeneity of rainfall along the path L. Only because $b \approx 1$ the measured attenuation can be related accurately to the path-averaged rain rate.

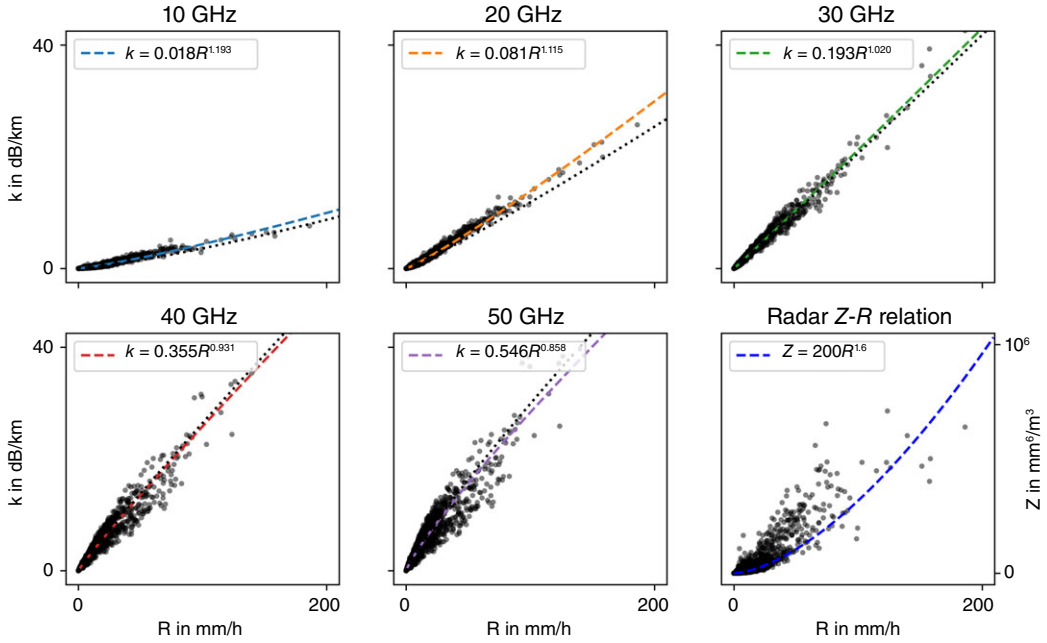

FIGURE 3 Plots of the relation between rain rate R and specific attenuation k for different frequencies in the microwave range and, for comparison, the relation between radar reflectivity Z and rain rate R. Each point represents a drop size distribution (DSD) of aggregated drop counts over 1 min, recorded by a *This Laser Disdrometer* from April till end of September of the years 2011, 2012, and 2013 in southern Germany. The DSD data has been filtered according to Friedrich, Kalina, Masters, and Lopez (2012). Calculations of k have been performed with the T-matrix method (Mishchenko, Travis, & Mackowski, 1996) for oblate spheroid shaped drops at 10°C using the Python package *pytmatrix* (Leinonen, 2014). The colored dashed lines represent a fit of the k-R relation. The dotted black lines follows the ITU recommendation (ITU, 2001). Striking is the very low DSD dependence of the k-R relation compared to the Z-R relation, in particular for the shown frequencies below 40 GHz. However, it has to be noted, that for low frequencies, for example, for 10 GHz, DSD dependence increases. Due to the equal scaling of all scatter plots, this is not easily visible from the figures

The cause for the linear nature of the k-R can be understood by looking at the specific $k(f)$ in dB/km for a certain frequency f and R in mm/hr as integrals of the DSD

$$R = 0.6 \times 10^{-3}\,\pi \int_D v(D) D^3 N(D)\, dD, \tag{3}$$

$$k(f) = 4.343 \times 10^{3} \int_D C_{\text{ext}}(D,f)\, N(D)\, dD, \tag{4}$$

where $N(D)$ is the DSD's number concentration per diameter in $\text{mm}^{-1}\text{m}^{-3}$, $v(D)$ is the falling rain drop's terminal velocity in m/s and $C_{\text{ext}}(D, f)$ is the extinction cross section at frequency f in m^2, which determines the attenuation an individual drop is causing. The integrands $C_{\text{ext}}(D, f)$ and $v(D)\,D^1$ have a very similar dependence on D, in particular for 20 GHz $< f <$ 35 GHz. As a result, k and R are nearly linearly related. Also, variations in the drop size distribution via deviations from the standard assumption for the shape of $N(D)$, only affect the k-R relation little. This lucky coincidence of telecommunication engineering needs (resulting in the typical CML frequencies) and scattering properties given by laws of physics make CMLs an accurate tool for rainfall estimation.

1.4 | A short retrospect on rain induced attenuation

1.4.1 | The early years of microwave transmission

In the 1930s, when radio communication technology was still limited to frequencies below 100 MHz, theoretical calculations already showed that rainfall would "markedly influence the propagation of waves less than 5 cm [6 GHz] in length" (Stratton, 1930). Only several years later, in 1946, the first empirical studies were presented that demonstrated the strong attenuating effect of rainfall in the frequency range from 10 to 50 GHz (Mueller, 1946; Robertson & King, 1946) indicating that "at the 1-cm wavelength, one can expect rather large path losses at the time of heavy or even moderate rains, particularly if the distances are large" (Robertson & King, 1946).

1.4.2 | The emergence of weather radars

Besides the field of radio communication, the attenuating effect of rainfall also drew attenuation from weather radar researchers. With the emerging usage of weather radars in the 1950s and the desire to quantify rainfall (Marshall, Langille, &

Palmer, 1947) it became apparent that attenuation also had to be considered as a potential error source (Hitschfeld & Bordan, 1954). But attenuation was not only considered as a potential error. It was radar researchers who, for the first time, realized that rain induced-attenuation can also be used to estimate rain rates, highlighting the low DSD dependence of the *A*-*R* relation (Atlas & Ulbrich, 1977). They also proposed several setups for attenuation measurement, for example, using fixed radar targets, dedicated receivers at a certain distance from the radar, and even a multi-reflector zig-zag path to retrieve areal integrated rainfall.

1.4.3 | The age of dedicated microwave transmission experiments

In the 1990s the upcoming Tropical Rainfall Measuring Mission (TRMM) and with it the need for reliable spatially averaged rainfall ground truth, triggered the development of a dedicated dual-polarization microwave transmission experiment. It was shown that differential attenuation measurements can be used to derive rainfall rates and are less prone to instrument fluctuations (Ruf, Aydin, Mathur, & Bobak, 1996). Later, a dual-frequency link was built to study the possibility of retrieving DSD information for TRMM ground validation. The DSDs retrieved by the dual-frequency inversion technique were in good agreement with in-situ observations (Rincon & Lang, 2002).

Driven by the fact that line-integrated microwave attenuation measurements, in contrast to rain gauge networks, provide continuous path-integrated rainfall information, led to the installation of four dedicated dual-frequency links (Rahimi, Holt, Upton, & Cummings, 2003). It was shown that reliable estimates of path-averaged rainfall can be derived from dual-frequency differential attenuation. In follow-up experiments, similar microwave links were used to distinguish rain and melting snow (Upton, Cummings, & Holt, 2007). A further analysis of a dedicated single-polarization single-frequency link, which was also used to measure evaporation via scintillometry, showed that correcting for wet antenna attenuation is crucial to avoid overestimating rain rates (Leijnse, Uijlenhoet, & Stricker, 2007b).

1.4.4 | The advent of cellular networks

The dedicated research microwave links showed that line-integrated attenuation measurements can provide reliable and valuable rainfall information. But scaling this new method up to cover larger areas would have meant installing another observation network in addition to the existing rain gauge and radar network.

Luckily, the steadily growing cellular networks, most prominently cell phone networks, use microwave links for a large part of their backhaul network. With the strong increase of cell phone users during the last 20 years, also the number of commercial microwave links (CMLs) increased dramatically, for example, from around 10,000 CMLs in Germany in 1996 to approximately 150,000 CMLs now (Ericsson, 2017).

Even though there was a considerable amount of CMLs available by the year 2000 the first empirical proof that rainfall estimation is also possible with CML attenuation data stems from 2006, using data from Israel (Messer, Zinevich, & Alpert, 2006). Shortly afterwards, analysis of CML data from the Netherlands further supported this finding (Leijnse, Uijlenhoet, & Stricker, 2007c).

2 | THE CHALLENGES OF PROCESSING RAINFALL FIELDS FROM RAW CML DATA

Figure 4 gives an overview of the workflow, starting with raw CML data and resulting in reconstructed rainfall fields. This section describes the individual steps, focusing on the general challenges that are involved. Details on the available solutions to tackle these challenges will be given in the next section on the state of the art.

2.1 | Unlocking and acquiring CML data

The first, and often most tedious, step is to access CML data. Since it stems from a network operated for a different purpose, there is no standard way of obtaining the data. In most cases, the CMLs record the required data, the transmitted signal level (TSL) and the received signal level (RSL) with a coarse temporal resolution for monitoring purposes. Most commonly the minimum and maximum for a period of 15 min is stored. But even if the data is technically available, the CML network operators, in most cases the large national cell phone providers, have no default processes to distribute the data. The crucial question typically is, how to identify the optimal contact person? Experience has shown that seeking a cooperation at a more technical level is more straightforward than accessing via the top levels of a company. With the demonstrated advances in CML rainfall estimations and its documented increasing usage in real-world applications, convincing CML operators to allow access to CML data hopefully gets easier in the future.

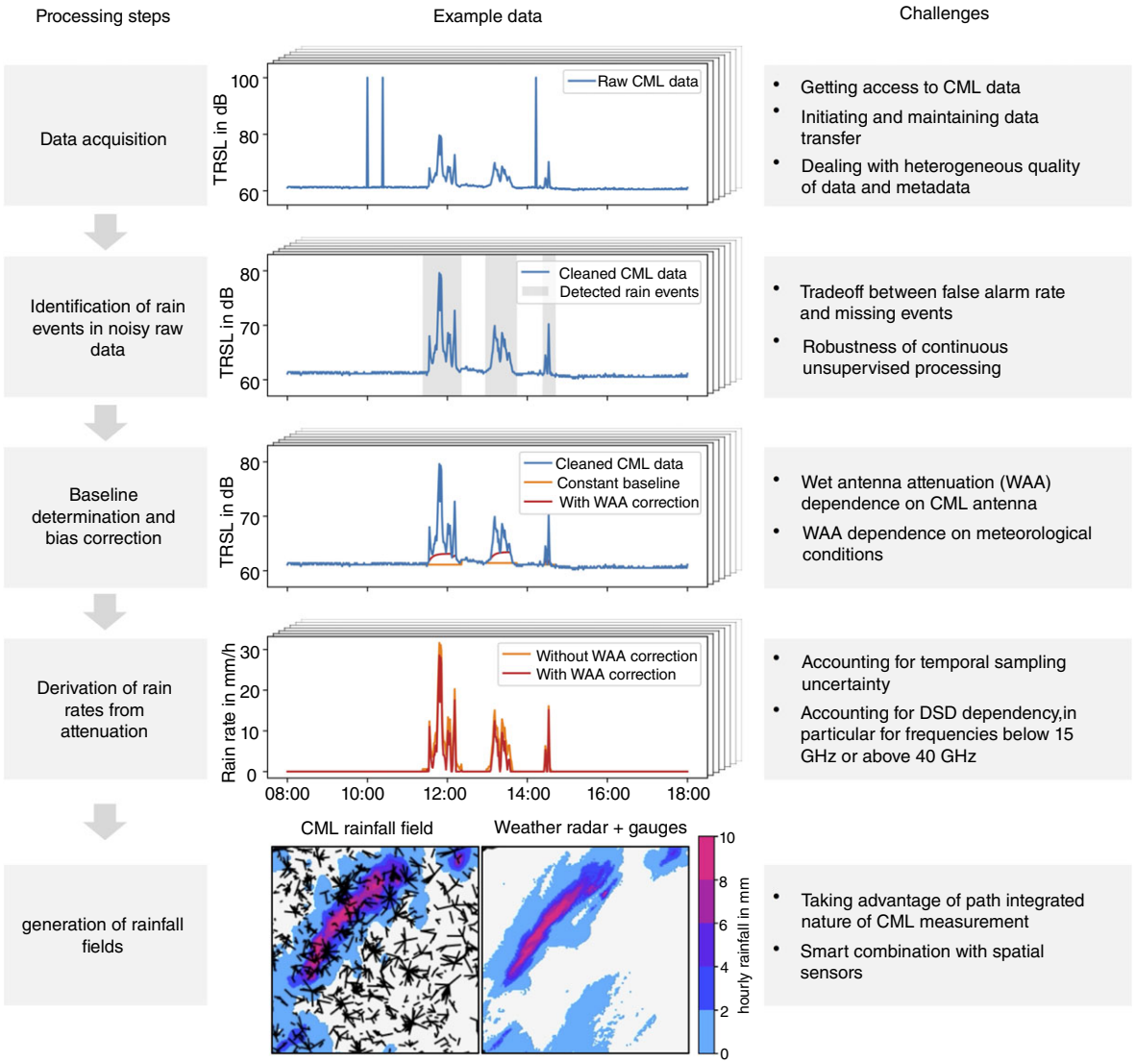

FIGURE 4 Illustration of a typical workflow, starting from acquiring several CML raw data time series to having CML-based rainfall fields. For better visibility of the details of the time series, the plots only show a very short time period of several hours. The black lines in the plot of the CML rainfall field represent the CML paths. Shown is the hourly rainfall sum compared to the hourly rain gauge adjusted weather radar product (RADOLAN-RW) of the German meteorological service (Chwala, Smiatek, & Kunstmann, 2018)

2.2 | Identification of rain events in noisy raw data

As can be seen in Figure 3 the relation between rain induced attenuation k and rain rate R is strong and robust. But rainfall is not the only cause for fluctuations of the signal levels. Changes in water vapor content and air temperature can lead to differences in propagation conditions. Air temperature changes or strong solar radiation can also lead to temperature-dependent drifts of the CML electronics in the transmitter and receiver. Furthermore, multi-path propagation, which exhibits rapidly changing propagation characteristics, can lead to large signal fluctuations at the receiver.

As a consequence, the total observed path attenuation is fluctuating even during clear sky conditions. Figure 5 shows fluctuations on different temporal scales for the same CML data set. The weekly median reveals a yearly cycle in the data, most probably stemming from higher average water vapor concentrations in summer, which lead to higher average attenuation. On a shorter temporal scale of hours, the excerpt of 3 days shows a similar but irregular diurnal pattern in the data. Since the strong fluctuations occur around midnight, they could be, but not necessarily are, attributed to the formation of a stable atmospheric boundary layer, which could potentially lead to significant changes in the propagation conditions. Figure 6 gives a more extreme example, with a CML that exhibits fluctuations during dry periods on the order of magnitude of strong precipitation events, up to 30 dB, equaling 40 mm/hr for this CML. The cause here is likely a strong multi-path problem, since the CML goes from one side of a large lake to the other. The second CML in Figure 6, with very low fluctuations during dry periods, is located directly in the vicinity but does not cross water.

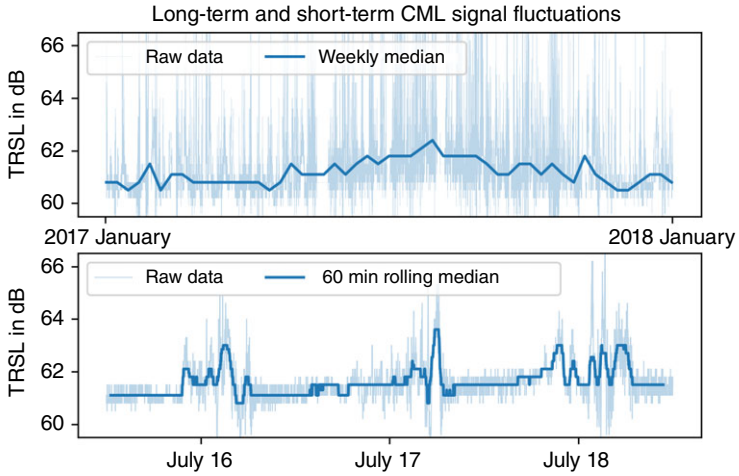

FIGURE 5 Example of a CML time series of the transmitted minus received signal level (TRSL) showing fluctuations on different temporal scales. (top) The weekly median clearly reveals a yearly pattern in the data. Note that the weekly median is used to filter influences from all the strong attenuation events, stemming from rainfall, which are visible in the raw data. (bottom) Example for a diurnal pattern of TRSL data, probably stemming from specific propagation characteristics during clear nights when a stable atmospheric boundary layer forms. Note that there was no rain present during the 3 days in July which are shown here. The data shown is the raw data which is sampled instantaneously every minute from a CML with a length of 19.6 km using a frequency of 16.4 GHz and vertical polarization

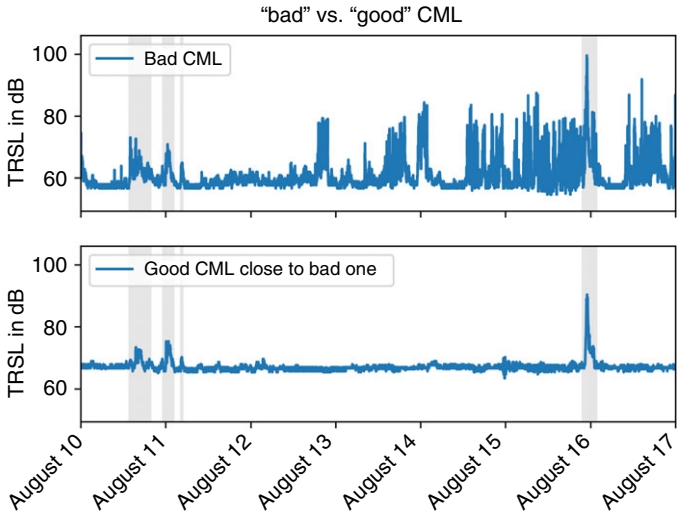

FIGURE 6 (top) Example of a CML which exhibits "bad" characteristics for rainfall estimation due to strong erratic fluctuations in its TRSL time series. These fluctuations most likely stem from multi-path propagation caused by reflections of the lake over which the CML path leads. (bottom) For comparison, data from a nearby CML with a fairly stable signal level during dry periods, which clearly reveals the rain events marked by the shaded period. The data shown is the raw data which is sampled instantaneously every minute. The "bad" CML has a length of 10.5 km and uses a frequency of 19.2 GHz with vertical polarization. The "good" CML has a length of 10.3 km and uses a frequency of 18.2 GHz with vertical polarization

The key challenge is to correctly detect also small rain events without having too much false alarms due to fluctuations during dry periods. For CMLs which exhibit large fluctuations this is particularly challenging. It might even be required to define upper thresholds and excluded CMLs from an analysis if fluctuations are above these thresholds. Fortunately, CMLs with strong multi-path effects are rare, though. They are not desirable for the CML operators because strong signal fluctuations lead to lower data transfer rates. Operators thus try to avoid paths, which are prone to multi-path effects, for example, leading over large water bodies.

In a continuous automated unsupervised processing workflow the detection of rain events is particularly challenging. A suitable method has to be fast enough to be applied in real-time, but is also has to be robust against unexpected fluctuations.

2.3 | Baseline determination and bias correction

After rain events have been detected in the CML data, the next step is to determine the baseline of the transmitted minus received signal level (TRSL), or baseline RSL if TSL is constant, which serves as a reference from which A is calculated.

Since the CMLs exhibit fluctuations during dry periods, it is also very likely that there will be fluctuations not caused by rain during the rainy period. However, since rain events are often short compared to the time scales of the signal fluctuations, one common assumption is that the baseline is constant during a rain event. Relying on this assumption is unsatisfactory, but the lack of additional information in the currently available CML data (with limited temporal and power resolution) does not allow to derive more information on the evolution of the baseline during a rain event. If future generations of CML hardware would provide data with higher resolution, spectral signal analysis might give more insight and enable us to distinguish between a slowly changing baseline and a much more variable rainfall signal.

Empirical data shows that rain drops on the antenna radome, so called wetting of the antenna, leads to additional attenuation, which leads to an overestimation of rain-induced attenuation and hence to an overestimation of rainfall. This additional attenuation, which can be on the order of several dB, can be parameterized and added to the baseline, compensating the overestimation.

2.4 | Derivation of rain rates from attenuation

Subtracting the baseline levels from the actual TRSL levels yields the rain-induced path-integrated attenuation A in dB which can be transformed into the path averaged rain rate $\bar{R}$ in mm/hr using Equation 2. If available, values of a and b for the local rainfall climate should be used. But since the DSD dependence of the k-R relation is low for frequencies between 15 and 35 GHz, the generalized values from the ITU recommendations (ITU, 2001) can also be applied if no local or regional DSD data is available for deriving adapted k-R parameters.

Depending on the temporal sampling of the CML data, A has to be corrected first, before being transformed into rain rates. E.g. the common 15-min minimum-maximum CML data will yield a $A_{\max}$ and a $A_{\min}$ from which an effective A must be derived, accounting for the probability distribution of rainfall within the 15 min an observation covers.

2.5 | Generation of rainfall fields

If several CMLs are available for a certain region, the path-averaged rain rates of each individual CML can be combined and used to derive spatial rainfall information. Several interpolation or reconstruction techniques can be used. Simple ones consider the CML data as point observation located in the middle of the CML path and use standard interpolation techniques for point data. This, however, discards the line-integrated nature of the CML observations. More sophisticated techniques use the full line-integrated information and therefore better constrain the spatial structure of the derive rainfall fields.

Due to the high spatial variability of rainfall, all interpolation and reconstruction methods are however limited. The shorter the temporal aggregation and the larger the distances between individual observations, the larger the errors and uncertainties of the resulting rainfall fields.

A further way to produce rainfall fields using CML data is to combine CMLs and a sensor that provides spatial information with the goal to mitigate uncertainty or bias of the spatial sensor. For example, rain rate estimates from weather radars might benefit from local adjustments via CML observations.

3 | STATE OF THE ART

3.1 | CML data availability in different countries

CML rainfall estimation is usually carried out on a national level because it always involves access to data of one of the national cell phone providers. Hence, for potential future collaborations, partners typically have to be found on a national level. Table 1 lists a selection of references to CML rainfall research sorted by country.

3.2 | CML data acquisition

To date, three different methods have been used for CML data acquisition (DAQ).

In most cases data from the *network management system* (NMS) systems has been used. Typically the NMS records the minimum and maximum TSL and RSL values at 15 min or hourly intervals. This data is used by the CML network operators to analyze errors or to identify problematic CMLs. Numerous publications have already proven that this min-max CML data can successfully be used for rainfall estimation also on a country-wide scale (Overeem, Leijnse, & Uijlenhoet, 2013; Zinevich, Alpert, & Messer, 2008). The temporal sampling rate is determined by the requirements of the CML network operators, though. To date, it is limited to 15 min or longer. The NMS data also quantizes the records of the power level, typically at 0.1, 0.3, or 1.0 dB steps, depending on the CML hardware, limiting the minimum detectable rain rate (see also Figure 7).

TABLE 1 A list of countries where CML data has been acquired and analyzed in a transparent and documented manner, either through publications or web visualizations

Country	Publication
Israel	Messer et al. (2006)
	Ostrometzky and Messer (2018)
Netherlands	Leijnse et al. (2007c)
	Rios Gaona et al. (2017)
Switzerland	Rieckermann, Lüscher, and Krämer (2009)
	Bianchi, Jan van Leeuwen, Hogan, and Berne (2013)
France	Schleiss and Berne (2010)
Germany	Chwala et al. (2012)
	Haese et al. (2017)
Luxembourg	Fenicia et al. (2012)
Kenya	Hoedjes et al. (2014)
Burkina Faso	Doumounia, Gosset, Cazenave, Kacou, and Zougmore (2014)
Czech Republic	Fencl, Rieckermann, Sýkora, Stránský, and Bareš (2015)
	Fencl, Valtr, Kvičera, and Bareš (2018)
Sweden	SMHI (2015)
Italy	D'Amico, Manzoni, and Solazzi (2016)
Brazil	Rios Gaona, Overeem, Raupach, Leijnse, and Uijlenhoet (2018)
Pakistan	Sohail Afzal, Shah, Cheema, and Ahmad (2018)

Note. For countries were more than one publication is available, only the first and the currently most recent one are listed.

In cases where data from the NMS is not available, data loggers directly at the CML towers can also be used to acquire data if an analog output related to the RSL levels is available. Acquiring data this way has the advantage that the temporal resolution can be chosen freely. Furthermore, the power resolution, that is, the quantization at which the signal levels are recorded, is not limited by the implementation of the NMS. Data in southern Germany was acquired this way with a power resolution of 0.025 dB as averages over 1 min. These advantages are, however, outweighed by the costs that this method would involve when scaled up to thousands of CMLs to extend the DAQ to cover a whole country. The data loggers are cheap, less than 100 Euro, but installation or maintenance work requires booking a technician with permission to work on the CML towers, easily reaching 1,000 Euro per day.

A way to have flexible temporal sampling without hardware installation is to use a custom software to poll the TSL and RSL levels inside the IP network containing the CMLs. TSL and RSL levels can be polled via the *simple network management protocol* (SNMP) from individual CMLs. Similar to the data provided by the NMS, the quantization of the TSL and RSL values is limited by the implementations on the individual CML hardware. This method has been used to acquire data from a dual-polarization CML operated for research purposes with a temporal resolution of 4 s (Wang, Schleiss, Jaffrain, Berne, & Rieckermann, 2012), but also has proven to be capable of acquiring data from numerous operational CMLs in the Czech Republic (Fencl et al., 2015). In Germany a custom open-source SNMP DAQ software (Chwala, Keis, & Kunstmann, 2016) is currently used to continuously acquire data from more than 4,000 CMLs country-wide in real time with a temporal resolution of 1 min. This DAQ software is hardware agnostic and is currently also operated for different CML hardware in Burkina Faso. A future application at a cell phone provider in Palestine is in preparation.

It should also be mentioned that it is not only crucial to acquire the TSL and RSL data, but also the CML metadata with information on locations, polarization and frequency. Errors in the metadata will unavoidably results in errors of the rainfall estimates (Rios Gaona et al., 2018).

With the numerous examples of successful CML data acquisition, unlocking data in new countries and from new cell phone providers hopefully will be more straightforward in the future.

3.3 | Rain event detection

For dealing with the fluctuations of the CML data (as shown in Figures 5 and 6) several methods have been developed. These methods can be distinguished into two classes.

One approach to identify rainy periods in the time series of CML data is to analyze the temporal correlation with time series from CMLs in the vicinity. This approach was successfully used to process 2 years of CML data for the entire

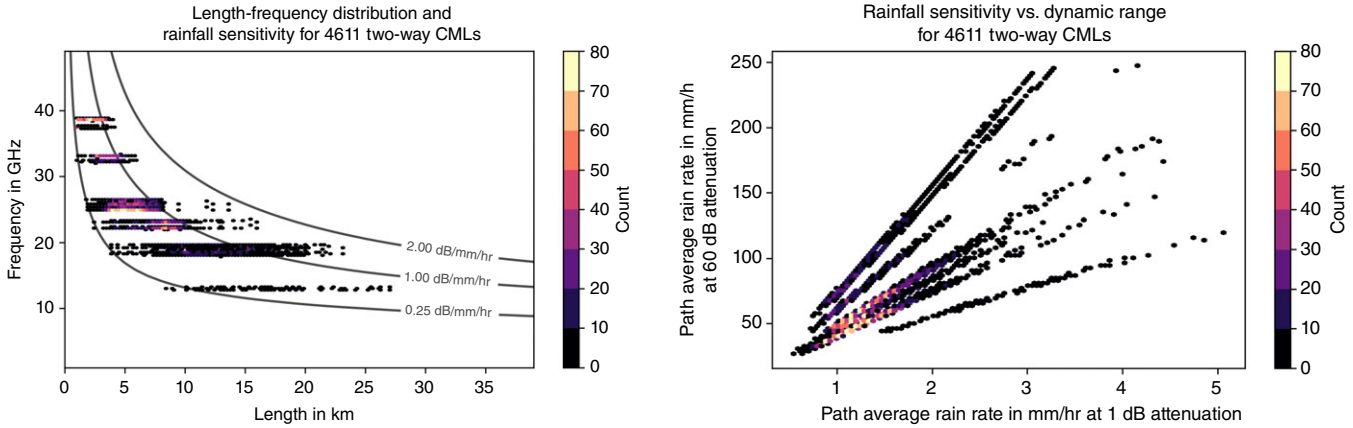

FIGURE 7 (left) Distribution of CML lengths and frequencies with their sensitivity to path-average rain rates. Clearly visible are the separated frequency bands which are used by CMLs. The sensitivity due to path-averaged rainfall (which is not taking into account possible variations along the CML path) increases with length and with higher frequencies. Hence, for most CMLs they are both chosen, so that the CML exhibits between 0.25 and 1.0 dB attenuation for a path-averaged rainfall rate of 1 mm/hr. (right) This figure shows the rain rate that causes 1 dB attenuation versus the rain rates that causes 60 dB attenuation at a specific CML. The values of the *x*- and *y*-axis can be interpreted as estimates of the minimum- and maximum detectable path averaged rain rate. It has to be noted, though, that the detection limit varies for each individual CML due to different quantization and different grades of noisiness of the TRSL records (e.g., as shown in Figures 5 and 6). The assumed dynamic range of 60 dB is a typical average value and might be different depending on the maximum available transmitter power

Netherlands (Overeem, Leijnse, & Uijlenhoet, 2016b). The implementation is available via the R-software package *RAINLINK* (Overeem, Leijnse, & Uijlenhoet, 2016a).

The second approach to distinguish between rainy and dry periods is to analyze the time series of individual CMLs separately. One method is to use a sliding-window standard deviation of the TRSL time series, which indicates rainy periods if this standard deviation is above a certain threshold (Schleiss & Berne, 2010). Similarly, Fourier transform power spectra of a sliding window of the time series can be used. The spectra of fluctuations during rainy periods exhibit a different behavior than the spectra during dry periods (Chwala et al., 2012). Both methods are available in the Python CML processing package *pycomlink*.[0] A further method for the detection of rainy periods in the time series is based on Markov switching models (Wang et al., 2012). Feasibility for the discrimination between rain- and sleet events, using a decision tree method with several classification features, has also been shown (Cherkassky, Ostrometzky, & Messer, 2014). For separating rainfall information from the fluctuating CML time series without a dedicated identification of rain events a simple approach which subtracts a rolling windowed minimum has been proposed (Ostrometzky & Messer, 2018).

In addition, preliminary results for the detection of rainy periods have been presented using artificial neural networks (Đorđević et al., 2013), random forest classifiers and gaussian factor graphs (Kaufmann & Rieckermann, 2011).

In general, the methods easily detect strong rain events, because these generate attenuation events a lot larger than the magnitude of the fluctuations during dry periods. The crux is distinguishing between small rain events and strong dry period fluctuations. All methods have to make a compromise between false positive and false negative detections. Since different CMLs may exhibit a very different severity of dry period fluctuations, the classification skill of a rain event detection methods cannot easily be transferred to another data set. Most existing methods have only been tested with a small dataset of several CMLs. The only long-term application to a large number of CMLs was carried out with data from 2044 CMLs for a 2.5 year period in the Netherlands using the *RAINLINK* algorithm described above, which was calibrated against gauge adjusted radar data for a 12 day period (Overeem et al., 2016b). Due to the lack of intercomparison studies, it is however not clear how the performance of the current methods compare to each other. It is not clear either how applicable the different methods are in new climatic regions, or for CMLs which just recently became available for rainfall estimation, or in regions without reliable rainfall ground truth where calibration of processing parameters is not possible.

As a consequence, this crucial step in the CML data processing workflow will need further research. With the steadily growing CML data sets and the rapidly evolving machine learning methods, many new possibilities arise to accomplish better performance in detecting light rain events. Small test data sets are available in *RAINLINK* (with distorted coordinates) and *pycomlink* (with fake coordinates). To support future research it would, however, be desirable to have at least one large open standard CML data set for benchmarking to be able to consistently judge the skill of newly developed methods.

3.4 | Min-max data processing

As mentioned in Section 3.2, CML data is often provided as records of the minimum and maximum RSL or TRSL over a given time. If this min-max data is used, an average rain rate value for the covered period must be derived to be able to compare with rainfall ground truth or to further use the CML-derived rainfall data, for example, in a hydrological model.

One option to do this is to take the average of a climatological probability distribution of rain rates clipped at the maximum and minimum rain rates derived directly from the maximum and minimum attenuation (Messer et al., 2006).

Another option is to apply a *k-R* power law to both the minimum and maximum signal level. The derived minimal and maximal rain rate can then be combined using a fixed weighted average. For the Dutch data set of 2044 CMLs over the period of 2.5 years, weighting factors of $\frac{1}{3}$ and $\frac{2}{3}$ for the maximum and minimum have been found to work best (Overeem et al., 2016b).

To date there is no study that evaluates the errors that the min-max sampling introduces compared to data that is instantaneously sampled at a higher rate.

3.5 | Identification of error sources and their mitigation

While the *k-R* relation is far more robust than the radar *Z-R* relation, other error sources limit the overall accuracy of rainfall estimation from CML attenuation data.

Potential sources for errors are: too coarse temporal sampling, quantization of TRSL values, uncertainty of the baseline level and wet antenna attenuation (Leijnse, Uijlenhoet, & Berne, 2010; Zinevich, Messer, & Alpert, 2010). The latter two dominate the overall error regarding the accuracy of the estimated rain rates. Hence, correct determination of the baseline and correction for wet antenna attenuation, in particular for insensitive CMLs (sensitivities are shown in Figure 7), are crucial processing steps. Additional uncertainty and bias is introduced by the variability of the rain rate and DSD along the CML paths (Berne & Uijlenhoet, 2007; Leijnse, Uijlenhoet, & Berne, 2010). As a consequence of Equation 2 the bias stemming from the spatial variability of the rain rate along the CML path is lowest for frequencies with a close to linear *k-R* relation. In general, this bias is also lower for shorter CML paths, for which the potential for rain rate variability along the path is lower. The uncertainties introduced by DSD variations along the CML path decrease with increasing length due to the averaging that occurs along the path (Leijnse, Uijlenhoet, & Berne, 2010).

Since the effect of wet antenna attenuation (WAA) is one of the dominant sources of error, several experiments were carried out to quantify its magnitude, study its dynamics and develop a suitable parameterization for it.

WAA can be modeled as a thin water film on the antenna with a uniform thickness (Blevis, 1965) which depends on the rain rate following a power law relation. This power law relation results in a rain rate dependent WAA, rising immediately with small rain rates (0–1 mm/hr) and leveling of towards high rain rates. Frequency dependence shows a slight peak around 22 GHz (Leijnse, Uijlenhoet, & Stricker, 2008). The assumption of a uniform water film allows analytic electromagnetic calculations of the WAA effect. However, real CML antennas do no show uniform wetting. Typically, either small droplets or runlets form on the antenna cover.

A rain rate dependence of the WAA effect was also found in sprinkler experiments for three CML antennas with different operating frequencies (Islam & Tharek, 2000). Similar sprinkler experiments (Kharadly & Ross, 2001) and long-term analysis of data from a dedicated single-CML (Minda & Nakamura, 2005) show similar results. Just recently the analysis of 2 years of data from very short CMLs (Fencl et al., 2018) concluded that the WAA effect shows a rain-rate-dependence and that it can reach up to 9 dB in extreme cases.

A different way to model the WAA is to assume a maximum WAA level and a time constant which determines how fast the modeled WAA approaches the maximum level over the course of a rain event (Schleiss, Rieckermann, & Berne, 2013). The model was derived with data from a setup with a 38 GHz CML over a path of 1.85 km. The maximum WAA level of this model that fitted the CML data best was found to be 2.3 dB. A method to calibrate the model using only the CML TRSL time series is also proposed. However, it was not yet shown that the proposed calibration procedure can be transferred to CMLs different from the one it was designed for.

Another way to account for variations of the baseline during rain events is to use a low-pass filter of the TRSL or RSL time series as baseline. This approach improved CML rainfall estimates compared to the processing with a constant baseline during the selected rain events (Fenicia et al., 2012). Although this approach was initially not intended to model the WAA effect, it might produce dynamics similar to the temporal evolution of an anticipated rain-rate-dependent WAA effect, where the baseline slowly follows the magnitude of the rain event.

If only the 15 min min-max CML data is available, the coarse data resolution does not allow for sophisticated dynamic WAA models. For rainfall estimation with a country-wide network of CMLs a pragmatic approach, subtracting a constant

WAA value of 2.3 dB from the TRSL levels, has been used to successfully match the CML rainfall rates to gauge corrected radar estimates (Overeem et al., 2013).

The challenge with transferability is that the WAA effect depends on specific CML antenna parameters. These parameters are, for example, the material of the antenna cover, the type of hydrophobic coating on the antenna cover or the aging of the hydrophobic coating. These differences cause very different dynamics of the WAA. On antennas with hydrophobic cover the water forms in beads which take much longer to evaporate than the thin films found on non-hydrophobic antenna covers (van Leth, Overeem, Leijnse, & Uijlenhoet, 2018). Furthermore, meteorological variables like air temperature, wind speed and relative humidity will affect the drying of the water on the antennas. A global calibration of WAA models, only depending on CML frequency, therefore does not seem possible.

Given the uncertainty due to the different wetting behaviors of the antenna covers, it is not surprising that the currently available WAA studies do not provide a conclusive picture. It remains unclear if a WAA model should be dependent on the rain rate (Fencl et al., 2018; Islam & Tharek, 2000; Kharadly & Ross, 2001; Leijnse et al., 2010) or not (Overeem et al., 2013; Schleiss et al., 2013) and if drying times should be in the order of minutes (Minda & Nakamura, 2005) or hours (Schleiss et al., 2013). In addition, it has to be considered that WAA might also be introduced by dew formation on the antennas (van Leth et al., 2018).

More detailed studies of the WAA effect for different types of CML antennas under different conditions would be required to better quantify the WAA effect and to be able to develop a model that can be applied without calibration via additional rainfall ground truth.

3.6 | Estimation of phenomena other than rain

Since rainfall is not the only cause for fluctuations in TRSL time series, it seems obvious to apply similar inversion techniques for other atmospheric quantities. Atmospheric water vapor content, in particular close to its resonance frequency at 22.235 GHz, attenuates microwave radiation. Similarly, fog also causes losses. For both, the estimation of water vapor content (David, Alpert, & Messer, 2009) and fog (David, Alpert, & Messer, 2013) from CML data, feasibility has been shown. However, the attenuating effect of water vapor and fog is small compared to the attenuating effect of rainfall. Hence, keeping in mind the challenges for rainfall estimation (coarse signal quantization of CML data, challenges for correctly detecting small rain events and challenges to correctly determine the baseline level), reliable applications of these methods over longer periods seem infeasible. A more sensitive proxy for water vapor content would be the phase delay experienced by microwave radiation along a path (Chwala, Kunstmann, Hipp, & Siart, 2014). Phase delay information is currently, however, not available from CMLs. With the trend to use higher and higher frequencies for CMLs, which is driven by the ever growing need for more bandwidth, future CML networks might become more sensitive to water vapor, though. Short CMLs using W-band (75–110 GHz) and D-band (110–170 GHz) might be common in the future (Ericsson, 2017). At these frequencies water vapor absorption is at least twice as strong as at the water vapor absorption line at 22.235 GHz, the most sensitive frequency in the current CML frequency band. The effective sensitivity of the future W-band and D-band CMLs to water vapor will, however, also depend on their path length.

Another approach to derive further information from the fluctuations of CML data is to relate fluctuations during dry periods (similar to the diurnal ones shown in Figure 5) to atmospheric temperature inversion (David & Gao, 2016). These inversions are prone to trap pollutants and hence might indicate periods of high likeliness for severe air pollution. The CML data can, however, not be used to detect air pollution by itself. The severity of the pollution, which might get trapped in an inversion that causes CML signal fluctuations, strongly depends on the presence of a pollution source, for example, traffic.

Given that CML attenuation data is sampled fast enough, for example, at 10 Hz, the CML fluctuations could however also be exploited to estimate evaporation (Leijnse, Uijlenhoet, & Stricker, 2007a) using the CMLs as so called scintillometer. Theoretically, CMLs should be able to provide attenuation data at this rate because the internal electronics processes the modulation of the CML signal, which is used to actually transfer data along the CML, with a much faster rate. But it is not clear if the data can be accessed at a rate of 10 Hz, for example, via SNMP or via another interface that would ideally also yield data with a finer quantization of the TRSL.

If CML data for two frequencies or two polarizations would be available simultaneously, potentially the methods from research carried out with dedicated dual-polarization or dual-frequency links could be applied (Rincon & Lang, 2002; Ruf et al., 1996; Upton et al., 2007). Currently these configurations are rare in CML networks, but, for example, combining data from different operators might provide the required diversity of CML configuration. Preliminary results from a dual-polarization CML showed that the estimation of a parameterized DSD is feasible, with limitations for low rain rates due to the CML signal quantization (Berne & Schleiss, 2009).

3.7 | Spatial interpolation and reconstruction

For many hydrometeorological applications, for example, spatially distributed hydrological models used in flood analysis, rainfall fields have to be provided. Therefore, spatial information has to be derived from the path-integrated CML observations.

The most simple approach is to represent each CML rainfall value as a virtual point observation in the middle of its path. The appropriateness of this simplification will depend on the length of the CMLs and the spatial variability of rainfall for the desired temporal aggregation. By using the point representation, any standard interpolation technique like inverse distance weighting (IDW) or ordinary kriging can be used to derive rainfall fields. For both methods the parameters should be adjusted according to the spatial covariance of rainfall. To avoid instabilities when deriving the parameters directly from the CML rainfall data, historic rain gauge data sets can be used. In the Netherlands, for example, the country-wide CML rainfall maps were derived via kriging using climatological semi-variograms extrapolated to the 15 min time step of the CMLs (Overeem et al., 2013). Further analysis of the uncertainties of kriging-based interpolation of CML rainfall observations showed that uncertainties stemming from the interpolation are small compared to uncertainties due to the derivation of rainfall information for each individual CML (Rios Gaona, Overeem, Leijnse, & Uijlenhoet, 2015).

To allow for variations of the rainfall rate along the CML paths during interpolation, an extended IDW method can be used. The CML path is split into several point observations for which the rain rate is redistributed iteratively until updates to the IDW interpolated field are below a certain threshold (Goldshtein, Messer, & Zinevich, 2009).

More sophisticated methods which can truly account for the path integrated nature of the CML measurements use tomographic reconstruction algorithms (D'Amico et al., 2016; Zinevich et al., 2008), Bayesian assimilation (Scheidegger & Rieckermann, 2014), stochastic reconstruction based on Copulas (Haese et al., 2017) or exploit the sparsity of rainfall fields (Roy, Gishkori, & Leus, 2016). But even the most sophisticated method cannot reproduce small scale rain events which have not been adequately detected because they occurred in a region with only very sparse, or without, CML coverage.

3.8 | Combination with other rainfall observation methods

CMLs provide certain advantages for rainfall observation compared to rain gauges or weather radars, for example, the robust k-R relation or the fact that the network is already installed and maintained. However, errors sources like the wet antenna effect (WAA) or the uncertainties associated with spatial interpolation, indicate that, if available, a combination with other rainfall sensors is advisable.

To adjust for the WAA bias of very short CMLs, often found in dense urban environments, CML rainfall estimates can be corrected with nearby rain gauge observations using temporally aggregated data (Fencl, Dohnal, Rieckermann, & Bareš, 2017). The other way around, CML rainfall information can be used to detect malfunctioning rain gauges (Bianchi, Rieckermann, & Berne, 2013).

If radar data is available, a weighted averaging scheme can be used to combine data of the different sensors to produce improved rainfall maps (Liberman, Samuels, Alpert, & Messer, 2014). In a more analytic way, CML data were also used to directly improve dual-polarization radar data processing by optimizing the relation between the radar's specific differential phase K_{dp} and the radar's attenuation (Trömel, Ziegert, Ryzhkov, Chwala, & Simmer, 2014).

More general frameworks for combining different rainfall sensors, that is, rain gauges, weather radar and CMLs, are provided by variational (Bianchi, Jan van Leeuwen, et al., 2013) or Bayesian methods (Scheidegger & Rieckermann, 2014). Stochastic reconstruction of rainfall fields, constrained by rain gauge and CML observations can also be used to generate ensembles of possible rainfall fields (Haese et al., 2017).

In addition to rain gauges and weather radars, CML data can be combined with satellite observations, for example, to infer rainy periods from cloud cover information (Schip et al., 2017). This combination will be beneficial in particular in developing countries, where rain gauge networks are sparse, weather radars are mostly not available, but improved rainfall observation methods are crucial. Concepts for flood early warning systems based on the combination of CML and satellite data already exist, for example, in Kenya (Hoedjes et al., 2014).

3.9 | Hydrometeorological applications

Hydrological modeling usually suffers from the uncertainty associated with the rainfall fields that are used to force the models. This is in particular true in urban environments and complex terrain where fast runoff process on small spatial scales dominate. An analysis of virtual CML observations, derived from synthetic DSD fields, showed that CLM rainfall estimates lead to improved dynamics of the modeled pipe flow in an urban drainage system for strong rain events (Fencl, Rieckermann, Schleiss, Stránský, & Bareš, 2013). Real CML observations where used for modeling runoff in an alpine catchment in southern Germany for a small flooding event. The combination of CML rainfall information with rain gauge data considerably

improved the model skill, compared to using gauge-adjusted radar or rain gauges alone (Smiatek, Keis, Chwala, Fersch, & Kunstmann, 2017). In contrast, the analysis of five distinct rainfall data sources via hydrological modeling of a small fairly flat catchment in the Netherlands did yield only little difference between gauge-adjusted radar and CML rainfall input (Brauer, Overeem, Leijnse, & Uijlenhoet, 2016). On the other hand, this also indicates that CML rainfall information can be on par with gauge-adjusted radar.

4 | DISCUSSION

4.1 | Current and future limitations

Assessing the state of the art, the following limitations of CML rainfall estimation can be identified to be most critical:

Limited data availability: The number of CMLs available for research has increased over the years, but given that hundreds of thousands of CMLs are installed in Europe, the few thousand that are currently included in the analysis do not allow to exploit the full potential. After all, one of the biggest benefits of CMLs is the huge available network. Continuous and fast data transfer is also still rare, making large-scale real-time applications impossible at this moment.

Bias due to noisy raw data: Signal level fluctuations during dry periods are erratic. CMLs with similar configurations can exhibit completely different behavior. Depending on the selection and eventual calibration of rain event detection methods in the noisy raw data, misclassifications can lead to over- or under-estimation of rainfall rates and rainfall sums. A compromise between false positives and false negatives has to be made. In particular, CMLs with strong or recurring fluctuations during dry periods can overestimate rainfall sums considerably if their noisiness is not accounted for because of frequent false positive rain events.

Bias due to wet antenna attenuation: Rain drops on the CML antennas lead to additional attenuation, resulting in an overestimation of rainfall. In particular insensitive CMLs, mostly the very short ones, suffer from this bias. Several methods for correction exists, but none was evaluated in detail for a large number of different types of CMLs with different antennas. It remains an open question how to consistently compensate the WAA effect for individual CMLs.

Lack of method intercomparisons: Almost all existing methods have been developed and tested with a specific data set, uniquely available to a dedicated research group. This is also due to the fact that sharing of CML data is restricted, since specific features, like geographic locations, might be considered sensitive information by the telecommunication providers. In most cases, the source code of the implementations is not available either. As a consequence, there has not yet been any dedicated intercomparison study, combining different methods and data sets.

These limitations can be overcome, or at least mitigated, by further research and extended collaboration with cell phone providers. There are, however, limitations of the CML rainfall estimation methods that are a direct result of the design of the CML networks and will persist in the future.

CML networks are constantly changing because of increasing demands for bandwidth or hardware upgrades. That is, CML networks can provide very valuable rainfall information for operational use or consistent records over a span of some years, but they cannot guarantee consistent long-term records.

Furthermore it has to be taken into consideration that engineers typically plan new CML paths according to a local or regional rainfall climatology so that they are available 99.999% of the time; that is, only 0.001% of the time (≈5 min per year) rain-induced attenuation will lead to a signal level too low for the receiver to correctly function. Length and frequency of the CMLs are chosen accordingly, as can be seen in the left plot in Figure 7. As a consequence, each CML has an upper and lower bound for rainfall estimation determined by its hardware parameters and path length. The plot on the right in Figure 7 gives an estimate of these bounds. It can be seen that detection limit and maximum range are opposing factors. Due to the diversity of CML configurations (length depends on requirements and topography, while available frequency bands are fixed) this fact could, however, be compensated by combining observations of neighboring CMLs with different sensitivities. Having access to CML networks of different cell phone providers, will certainly increase this diversity.

The spatial distribution of CMLs is of course not determined by the needs for rainfall estimation. The density of CMLs correlates strongly with population density (Overeem et al., 2013), simply because a higher number of cell phone users requires a denser network of cell phone base stations. As a consequence, CML density is high in cities, highlighting their potential for urban drainage applications. In rural areas the density is lower. As can be seen from Figure 2, in a country like France regions without CML coverage are rare, though. In similarly developed and populated countries the situation is probably very similar. However, in regions which are only sparsely populated, for example, like in large parts of Canada, Amazonia or in desert regions, cell phone coverage is typically non existent (Overeem et al., 2016b) and thus CMLs most probably do not exist either or might only be available in individual larger settlements.

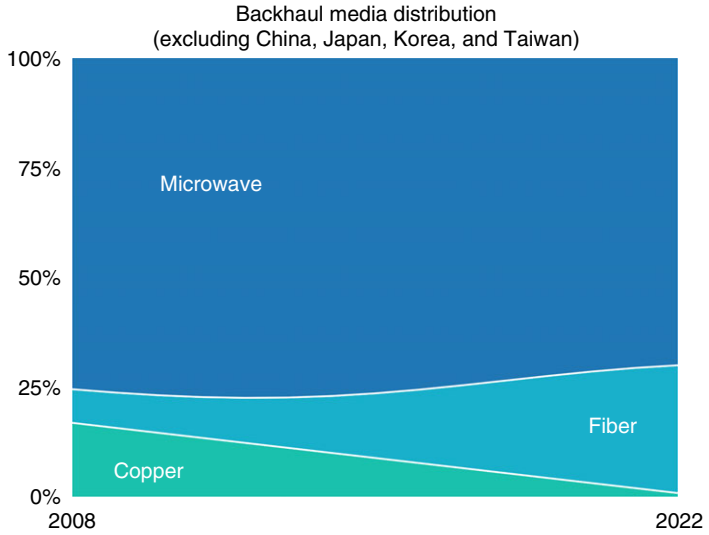

FIGURE 8 Predicted worldwide evolution of the usage of microwave links, fiber optics and copper wires in the cell phone backhaul. Based on data from Ericsson (2017)

4.2 | Future potential

With the increased usage of fiber optic communication in the cell phone backhaul networks, the question arises, whether CML data will still be available in the future. Indeed, as shown in Figure 8, the fraction of fiber-based backhaul connections is projected to increase over the next years. The dynamic evolution of the cell phone networks will, however, still favor CMLs due to their rapid deployment. Even though the fraction of CMLs will decrease in favor of fiber optics, the further upgrades of the cell phone networks, will increase the total number of backhaul installations. Hence, overall the number of installed CMLs will likely continue to increase. Depending on existing fiber optics infrastructure, there will be regional and national differences, though.

In particular in Africa the number of CMLs will likely increase in the future. As can be seen in Figure 9, Africa still has and will most likely continue to have a rapid increase of cell phone users. The fast evolution of the cell phone market there, paired with the low prevalence of fiber optics installation, will very likely result in an increased density of CMLs. This fits perfectly with the initiatives to advance CML rainfall estimation in the many water-sensitive regions of Africa (Gosset et al., 2016). Since CML rainfall maps have been shown to outperform satellite observations, namely in case of the GPM (global precipitation measurement mission) IMERG final run (Rios Gaona et al., 2017), and since satellite observations are in most cases the only promptly available rainfall information in African countries, hydrometeorological applications there will benefit most from the addition of CML rainfall estimation.

For regions with good weather radar coverage, like in most parts of Europe, a combination of CMLs and radars will be most beneficial. This is in particular true for urban regions and complex terrain, where ground clutter and beam blockage limit radar rainfall accuracy. In exactly these regions the potentially high temporal resolution and real-time availability of CML data will also help to improve nowcast and short term forecasts of the prevailing fast runoff processes.

4.3 | Future challenges

To advance the state of the art and make the proclaimed potential applications possible in the future, the following *scientific challenges* have to be tackled:

Robust continuous data processing: To be able to cope with the increasing amount of CML data and to advance CML rainfall estimation towards operational use, future processing methods must be able to robustly filter out the erratic fluctuations that CML data can exhibit. Only this way continuous and potentially unsupervised processing, in particular identification of rainy periods, can be carried out.

Reliable compensation of the wet antenna attenuation (WAA) effect: Correcting the WAA effect for different CMLs with different types of antennas is key to reduce biases in the CML rainfall estimates. More empirical studies with different real CML antennas will be required to get a better idea of the transferability of correction methods. It will however be crucial to

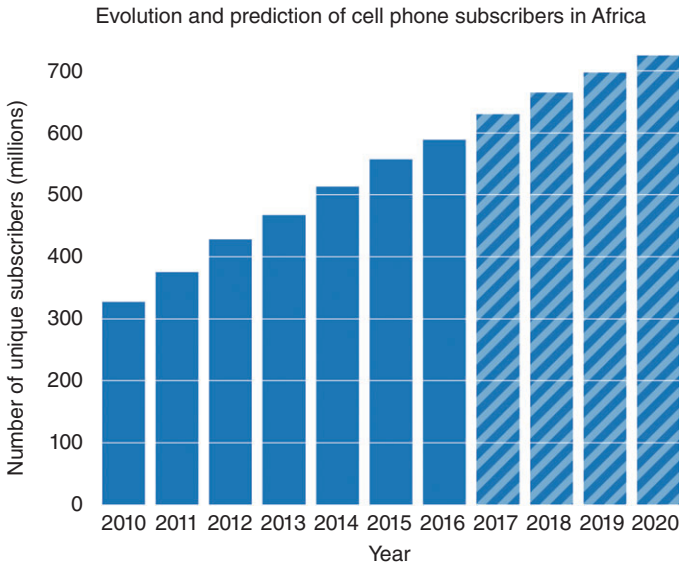

FIGURE 9 Shown are the numbers of cell phone subscribers in Africa for the last years (solid bars) and the predicted evolution till 2020 (hatched bars). Based on data from GSMA (2016)

integrate meteorological parameters into the equation. Albeit very ambitious, a unified WAA correction method that models the potential WAA variability during a rain event should be envisaged.

Continuous combination with radar or satellite data: Spatial interpolation always implies uncertainties. This holds also true for rainfall fields that are derived from the line-integrated CML rainfall information. Hence, combination with spatial sensors like weather radars or weather satellites should be aimed at, advancing the existing methods. Performing the combination of radar and CMLs continuously, for example, to bring the improved CML rainfall information to operational flood nowcasting, will not only be a scientific challenge, but also a strategic one, due to challenges in data acquisition and data sharing.

Method intercomparisons: One or more large standard CML data sets should be compiled and used for intercomparing the available methods. This would be facilitated if the source code of the individual methods always is available.

CML rainfall estimation is only possible because of, and together with, the commercial companies that operate the CML networks. Hence, there are also future *strategic challenges*:

Extension of data acquisition: Only a fraction of the installed CMLs are available for rainfall estimation and an even smaller fraction is continuously available. CML network operators hence have to be convinced, for example, via support from the GSM Association (GSMA) or the International Telecommunication Union (ITU), to further commit to this technique, extending CML data acquisition and allowing continuous data transfer. It is also crucial to have correct metadata (location, frequency, polarization) for each CML, to avoid severe errors in the derived rainfall estimates.

Monetization of CML data: It is clear that extended, continuous and guaranteed data acquisition cannot be provided by the CML operators free of charge. Discussions need to be initiated to negotiate the most beneficial pathway for monetization of CML data. One of the central advantages of CMLs is the existence of large redundant networks. Hence, bringing data from several CML network operators together generates the biggest scientific and societal benefit. Competing solutions for data monetization from different companies can probably not provide that. On the other hand, it is not foreseeable how many CML network operators are willing to engage in this topic. In the end, having one working CML-operator-specific solution is better than having a potentially unifying but unfulfilled promise.

Guideline for data sharing: Extended usage of CML data will require to clearly define the constraints for data sharing. With the growing demand, and also growing pressure due national and international (European) legislation, to openly share data associated with published research results, this issue is in particular important for scientists. If possible, global or national guidelines for CML data sharing should be developed to avoid detailed legal negotiations with individual CML network operators.

Our vision for an ideal world regarding data for CML rainfall estimation would be to have joint national data repositories to which all CML network operators continuously push their data. Historic data could be accessed openly, while real-time data is restricted for hydro-meteorological services or dedicated customers. The efforts to acquire and transfer CML data to the central repository would be compensated for, for example, by the number of observations transferred per time (Box 1).

BOX 1

CML RAINFALL COMMUNITY EFFORTS

Despite having no official central platform yet, the CML rainfall community is already collaborating to jointly advance the research field of CML rainfall estimation. The Winter School hosted by KIT in 2012[1] was the first effort to bring the community together, to discuss research and to teach the individual methods to young researchers. The jointly organized *Rain Cell Africa* workshop, held in Ouagadougou (Burkina Faso) in 2015, was the next step, promoting this new technique in one of the regions where its future implementation has the largest potential (Gosset et al., 2016). At a jointly held training workshop at the International Conference for Urban Drainage (ICUD), potential future users from the urban drainage community were introduced to CML data processing via hands-on programming exercises.

Efforts to make the developed methods openly available also already exist. The source code used for processing and producing country-wide rainfall maps from CML data in the Netherlands is available via the R package *RAINLINK* (Overeem et al., 2016a). The open source Python package *pycomlink*[3] provides several of the published methods for CML data processing to realize different workflows for the generation of rainfall maps. To ease future data exchange of CML data, a preliminary data format standard called *cmlh5*, based on the HDF5 format, has been elaborated.

In addition, community members are continuously helping to unlock and process CML data in new regions, for example, West Africa and the Middle-East, where water stress is a current and future challenge.

RAINFALL AND THE UPCOMING 5G NETWORKS

The 5th generation wireless system (5G) will be rolled out by cell phone providers in the next years, with some already ongoing pilots in selected cities. 5G will not only change the CML backhaul due to the higher bandwidth requirements. It will also bring a massive change in the frequency used for the connection between cellphones and base stations. The new high bandwidth spectrum for mobile devices is foreseen to be at 26 GHz. That is, similarly to CMLs, 5G cell phones will experience strong attenuation by rain. As a consequence the switch to 5G could yield an enormous amount of attenuation data potentially usable for rainfall estimation. Each 5G cell phone using the new high bandwidth spectrum could act as rainfall sensor.

The challenge to separate rainfall information from this huge hypothetical amount of data will be huge, too. Cell phones, compared to CMLs, are mostly non stationary. Connections between cell phones and base stations will not only be line of sight. The radiation will strongly interact with the environment, for example, through reflection or diffraction from buildings. And in addition, 5G cell phones will most likely have dynamically adjusted antennas, using beam forming and beam steering, to reach required the high antenna gain levels. The transmitted signal level will thus be highly variable.

Given that the identification of rain events, in particular small ones, in CML attenuation time series is already challenging, 5G data will take this challenge an order of magnitude further. On the other hand, the amount and diversity of the data paired with machine learning and computing power might make it possible to filter out the relevant information. The knowledge gained from analyzing CML attenuation data will certainly help. We will find out when we get access to the first 5G attenuation data.

5 | CONCLUSION

CML rainfall estimation has come a long way since the first published results in 2006. With the advancements in processing methods the derived rainfall information can compete with the quality of gauge-adjusted radar data. The potential for applications, for example, for flood forecasting, has already been shown. With the further increase of the number of installed CMLs, in particular in Africa, this technique can provide crucial rainfall information for water-sensitive regions.

Several hurdles have to be overcome to unlock the full potential of this technique, though. Accessing CML data is still limited and cumbersome, while the current processing methods cannot reliably compensate the biases introduced through the fluctuating CML signals and the effect of wet antenna attenuation.

Nevertheless, CML rainfall estimation has gained more and more momentum during the past years, with an increasing number of active researches and unlocked CML data from new countries. This shows that CML rainfall research is becoming an established field in hydrometeorology. We hope that our analysis of the current state of the art and our outlined opinion on

future options and challenges may serve as a useful guideline for continuing this exciting and emerging field of societally relevant research.

ACKNOWLEDGMENTS

We thank Remko Uijlenhoet and the anonymous reviewer for the many critical and constructive comments during the revision process, which helped to improve the quality of this review paper. Furthermore we are grateful for the continuous support from Ericsson Germany who helped initializing CML data acquisition in Germany and who allow us to acquire and analyze CML data on a country-wide scale. This work was supported by funds from the German Research Foundation (DFG) within the project *Integrating Microwave Link Data For Analysis of Precipitation in Complex Terrain: Theoretical Aspects and Hydrometeorological Applications (IMAP).* We also would like to thank the Helmholtz Association of German Research Centers for funding the initial CML rainfall research in Germany via the project *Regional Precipitation Observation by Cellular Network Microwave Attenuation and Application to Water Resources Management (PROCEMA).*

CONFLICT OF INTEREST

The authors have declared no conflicts of interest for this article.

ENDNOTES

[1]https://github.com/pycomlink/pycomlink

[2]https://www.imk-ifu.kit.edu/downloads/institute/KIT_WinterSchoolFeb2012.pdf

[3]https://lafibre.info/faisceau-hertzien/cartographie-des-faisceaux-hertziens

RELATED WIREs ARTICLE

Increasing river floods: Fiction or reality?

REFERENCES

Andrieu, H., Creutin, J. D., Delrieu, G., & Faure, D. (1997). Use of a weather radar for the hydrology of a mountainous area. Part I: Radar measurement interpretation. *Journal of Hydrology*, *193*(1–4), 1–25.

Atlas, D., & Ulbrich, C. W. (1977). Path- and area-integrated rainfall measurement by microwave attenuation in the 1-3 cm Band. *Journal of Applied Meteorology*, *16* (12), 1322–1331.

Berg, P., Moseley, C., & Haerter, J. O. (2013). Strong increase in convective precipitation in response to higher temperatures. *Nature Geoscience*, *6*(3), 181–185. https://doi.org/10.1038/ ngeo1731

Berne, A., & Krajewski, W. (2013). Radar for hydrology: Unfulfilled promise or unrecognized potential? *Advances in Water Resources*, *51*, 357–366.

Berne, A., & Schleiss, M. (2009). Retrieval of the rain drop size distribution using telecommunication dual-polarization microwave links. In *34th conference on radar meteorology*, American Meteorological Society, Boston.

Berne, A., & Uijlenhoet, R. (2007). Path-averaged rainfall estimation using microwave links: Uncertainty due to spatial rainfall variability. *Geophysical Research Letters*, *34*, L07403. https://doi.org/10.1029/2007GL029409

Bianchi, B., Jan van Leeuwen, P., Hogan, R. J., & Berne, A. (2013). A variational approach to retrieve rain rate by combining information from rain gauges, radars, and microwave links. *Journal of Hydrometeorology*, *14*(6), 1897–1909. https://doi.org/10.1175/JHM-D-12-094.1

Bianchi, B., Rieckermann, J., & Berne, A. (2013). Quality control of rain gauge measurements using telecommunication microwave links. *Journal of Hydrology*, *492*, 15–23. https://doi.org/10.1016/j.jhydrol.2013.03.042

Blevis, B. (1965). Losses due to rain on radomes and antenna reflecting surfaces. *IEEE Transactions on Antennas and Propagation*, *13*(1), 175–176. https://doi.org/10.1109/ TAP.1965.1138384

Brauer, C. C., Overeem, A., Leijnse, H., & Uijlenhoet, R. (2016). The effect of differences between rainfall measurement techniques on groundwater and discharge simulations in a lowland catchment. *Hydrological Processes*, *30*(21), 3885–3900. https://doi.org/10.1002/ hyp.10898

Cherkassky, D., Ostrometzky, J., & Messer, H. (2014). Precipitation classification using measurements from commercial microwave links. *IEEE Transactions on Geoscience and Remote Sensing*, *52*(5), 2350–2356. https://doi.org/10.1109/TGRS.2013.2259832

Chwala, C., Gmeiner, A., Qiu, W., Hipp, S., Nienaber, D., Siart, U., … Kunstmann, H. (2012). Precipitation observation using microwave backhaul links in the alpine and pre-alpine region of Southern Germany. *Hydrology and Earth System Sciences*, *16*(8), 2647–2661. https://doi.org/10.5194/hess-16-2647-2012

Chwala, C., Keis, F., & Kunstmann, H. (2016). Real-time data acquisition of commercial microwave link networks for hydrometeorological applications. *Atmospheric Measurement Techniques*, *9*(3), 991–999. https://doi.org/10.5194/amt-9-991-2016

Chwala, C., Kunstmann, H., Hipp, S., & Siart, U. (2014). A monostatic microwave transmission experiment for line integrated precipitation and humidity remote sensing. *Atmospheric Research*, *144*, 57–72. https://doi.org/10.1016/j.atmosres.2013.05.014

Chwala, C., Smiatek, G., & Kunstmann, H. (2018). Real-time country-wide rainfall derived from a large network of commercial microwave links in Germany. In *EGU general assembly conference abstracts*, European Geoscience Union, Munich, Germany (Vol. 20, p. 10096). https://meetingorganizer.copernicus.org/EGU2018/EGU2018-10096.pdf

D'Amico, M., Manzoni, A., & Solazzi, G. L. (2016). Use of operational microwave link measurements for the tomographic reconstruction of 2-D maps of accumulated rainfall. *IEEE Geoscience and Remote Sensing Letters*, *13*(12), 1827–1831. https://doi.org/10.1109/LGRS.2016.2614326

David, N., Alpert, P., & Messer, H. (2009). Technical note: Novel method for water vapor monitoring using wireless communication networks measurements. *Atmospheric Chemistry and Physics*, *9*, 2413–2418.

David, N., Alpert, P., & Messer, H. (2013). The potential of commercial microwave networks to monitor dense fog-feasibility study. *Journal of Geophysical Research: Atmospheres*, *118*, 11,750–11,761. https://doi.org/10.1002/2013JD020346

David, N., & Gao, H. O. (2016). Using cellular communication networks to detect air pollution. *Environmental Science & Technology*, *50*(17), 9442–9451. https://doi.org/10.1021/ acs.est.6b00681

Đorđević, V., Pronić-Rančić, O., Marinković, Z., Milijić, M., Marković, V., Siart, U., … Kunstmann, H. (2013). New method for detection of precipitation based on artificial neural networks. *Microwave Review*, *19*(2), 50–55.

Doumounia, A., Gosset, M., Cazenave, F., Kacou, M., & Zougmore, F. (2014). Rainfall monitoring based on microwave links from cellular telecommunication networks: First results from a West African test bed. *Geophysical Research Letters*, *41*(16), 6016–6022. https://doi.org/10.1002/2014GL060724

Ericsson. (2017). *Ericsson Microwave outlook—Trends and needs in the Microwave industry*. Retrieved from https://www.ericsson.com/assets/local/microwave-outlook/documents/ericsson-microwave-outlook-report-2017.pdf.

Fencl, M., Dohnal, M., Rieckermann, J., & Bareš, V. (2017). Gauge-adjusted rainfall estimates from commercial microwave links. *Hydrology and Earth System Sciences*, *21*(1), 617–634. https://doi.org/10.5194/hess-21-617-2017

Fencl, M., Rieckermann, J., Schleiss, M., Stránský, D., & Bareš, V. (2013). Assessing the potential of using telecommunication microwave links in urban drainage modelling. *Water Science & Technology*, *68*(8), 1810–1818. https://doi.org/10.2166/wst.2013.429

Fencl, M., Rieckermann, J., Sýkora, P., Stránský, D., & Bareš, V. (2015). Commercial microwave links instead of rain gauges: fiction or reality? *Water Science and Technology*, *71*(1), 31–37. https://doi.org/10.2166/wst.2014.466

Fencl, M., Valtr, P., Kvičera, M., & Bareš, V. (2018). Quantifying wet antenna attenuation in 38-ghz commercial microwave links of cellular backhaul. *IEEE Geoscience and Remote Sensing Letters*. https://ieeexplore.ieee.org/abstract/document/8525284

Fenicia, F., Pfister, L., Kavetski, D., Matgen, P., Iffly, J.-F., Hoffmann, L., & Uijlenhoet, R. (2012). Microwave links for rainfall estimation in an urban environment: Insights from an experimental setup in Luxembourg-City. *Journal of Hydrology*, *464˙465*, 69–78. https://doi.org/10.1016/j.jhydrol.2012.06.047

Friedrich, K., Kalina, E. A., Masters, F. J., & Lopez, C. R. (2012). Drop-size distributions in thunderstorms measured by optical disdrometers during VORTEX2. *Monthly Weather Review*, *41*, 1182–1203. https://doi.org/10.1175/MWR-D-12-00116.1

Goldshtein, O., Messer, H., & Zinevich, A. (2009). Rain rate estimation using measurements from commercial telecommunications links. *IEEE Transactions on Signal Processing*, *57*(4), 1616–1625. https://doi.org/10.1109/TSP.2009.2012554

Gosset, M., Kunstmann, H., Zougmore, F., Cazenave, F., Leijnse, H., Uijlenhoet, R., … Hoedjes, J. (2016). Improving rainfall measurement in gauge poor regions thanks to mobile telecommunication networks. *Bulletin of the American Meteorological Society*, *97*(3), ES49–ES51. https://doi.org/10.1175/BAMS-D-15-00164.1

GSMA. (2016). The Mobile Economy—Africa 2016. Retrieved from https://www.gsma.com/mobileeconomy/africa/.

Haese, B., Hörning, S., Chwala, C., Bárdossy, A., Schalge, B., & Kunstmann, H. (2017). Stochastic reconstruction and interpolation of precipitation fields using combined information of commercial microwave links and rain gauges. *Water Resources Research*, *53*(12), 10740–10756. https://doi.org/10.1002/2017WR021015

Hazenberg, P., Leijnse, H., & Uijlenhoet, R. (2011). Radar rainfall estimation of stratiform winter precipitation in the Belgian Ardennes. *Water Resources Research*, *47*, W02507. https://doi.org/10.1029/2010WR009068

Hitschfeld, W., & Bordan, J. (1954). Errors inherent in the radar measurement of rainfall at attenuating wavelengths. *Journal of Meteorology*, *11*(1), 5867.

Hoedjes, J. C. B., Kooiman, A., Maathuis, B. H. P., Said, M. Y., Becht, R., Limo, A., … Su, B. (2014). A conceptual flash flood early warning system for Africa, based on terrestrial microwave links and flash flood guidance. *ISPRS International Journal of Geo-Information*, *3*(2), 584–598. https://doi.org/10.3390/ijgi3020584

Hou, A. Y., Kakar, R. K., Neeck, S., Azarbarzin, A. A., Kummerow, C. D., Kojima, M., … Iguchi, T. (2013). The global precipitation measurement mission. *Bulletin of the American Meteorological Society*, *95*(5), 701–722. https://doi.org/10.1175/BAMS-D-13-00164.1

Islam, M. R., & Tharek, A. R. (2000). Measurement of wet antenna effect on microwave propagation at 23, 26 and 38 GHz. In *IEEE Antennas and Propagation Society International Symposium. Transmitting Waves of Progress to the Next Millennium, 2000 Digest. Held in conjunction with: USNC/URSI National Radio Science Meeting*, Salt Lake City, UT (Vol. 4, pp. 2094–2098). https://doi.org/10.1109/APS.2000.874906

ITU. (2001). *ITU-R P.676-9: Attenuation by atmospheric gases*. Geneva, Switzerland: International Telecommunication Union.

Kaufmann, M., & Rieckermann, J. (2011). Identification of dry and rainy periods using telecommunication microwave links. In *12nd International Conference on Urban Drainage, Porto Alegre/Brazil*, London: International Water Association (pp. 10–15).

Kharadly, M., & Ross, R. (2001). Effect of wet antenna attenuation on propagation data statistics. *IEEE Transactions on Antennas and Propagation*, *49*(8), 1183–1191. https://doi.org/10.1109/8.943313

Leijnse, H., Uijlenhoet, R., & Berne, A. (2010). Errors and uncertainties in microwave link rainfall estimation explored using drop size measurements and high-resolution radar data. *Journal of Hydrometeorology*, *11*(6), 1330–1344. https://doi.org/10.1175/ 2010JHM1243.1

Leijnse, H., Uijlenhoet, R., & Stricker, J. (2008). Microwave link rainfall estimation: Effects of link length and frequency, temporal sampling, power resolution, and wet antenna attenuation. *Advances in Water Resources*, *31*(11), 1481–1493. https://doi.org/10.1016/ j.advwatres.2008.03.004

Leijnse, H., Uijlenhoet, R., & Stricker, J. N. M. (2007a). Hydrometeorological application of a microwave link: 1. Evaporation. *Water Resources Research*, *43*, W04416. https://doi.org/10.1029/2006WR004988

Leijnse, H., Uijlenhoet, R., & Stricker, J. N. M. (2007b). Hydrometeorological application of a microwave link: 2. Precipitation. *Water Resources Research*, *43*, W04417. https://doi.org/10.1029/2006WR004989

Leijnse, H., Uijlenhoet, R., & Stricker, J. N. M. (2007c). Rainfall measurement using radio links from cellular communication networks. *Water Resources Research*, *43*, W03201. https://doi.org/10.1029/2006WR005631

Leijnse, H., Uijlenhoet, R., van de Beek, C. Z., Overeem, A., Otto, T., Unal, C. M. H., … Holleman, I. (2010). Precipitation measurement at CESAR, The Netherlands. *Journal of Hydrometeorology*, *11*(6), 1322–1329. https://doi.org/10.1175/2010JHM1245.1

Leinonen, J. (2014). High-level interface to T-matrix scattering calculations: Architecture, capabilities and limitations. *Optics Express*, *22*(2), 1655–1660. https://doi.org/10.1364/OE.22.001655

Liberman, Y., Samuels, R., Alpert, P., & Messer, H. (2014). New algorithm for integration between wireless microwave sensor network and radar for improved rainfall measurement and mapping. *Atmospheric Measurement Techniques*, *7*(10), 3549–3563. https://doi.org/10.5194/ amt-7-3549-2014

Marshall, J. S., Langille, R. C., & Palmer, W. M. (1947). Measurement of rainfall by radar. *Journal of the Atmospheric Sciences*, *4*(6), 186–192.

Messer, H., Zinevich, A., & Alpert, P. (2006). Environmental Monitoring by Wireless Communication Networks. *Science*, *312*(5774), 713. https://doi.org/10.1126/ science.1120034

Minda, H., & Nakamura, K. (2005). High temporal resolution path-average rain gauge with 50-GHz band microwave. *Journal of Atmospheric and Oceanic Technology*, *22*(2), 165–179.

Mishchenko, M. I., Travis, L. D., & Mackowski, D. W. (1996). T-matrix computations of light scattering by nonspherical particles: A review. *Journal of Quantitative Spectroscopy and Radiative Transfer*, *55*(5), 535–575. https://doi.org/10.1016/0022-4073(96)00002-7

Mueller, G. (1946). Propagation of 6-millimeter waves. *Proceedings of the IRE*, *34*(4), 181–183. https://doi.org/10.1109/JRPROC.1946.234240

Nešpor, V., & Sevruk, B. (1999). Estimation of wind-induced error of rainfall gauge measurements using a numerical simulation. *Journal of Atmospheric and Oceanic Technology*, *16*, 450–464.

Ostrometzky, J., & Messer, H. (2018). Dynamic determination of the baseline level in microwave links foer rain monitoring from minimum attenuation values. *IEEE Journal of Selected Topics in Applied Earth Observations and Remote Sensing*, *11*(1), 24–33. https://doi.org/10.1109/JSTARS.2017.2752902

Overeem, A., Leijnse, H., & Uijlenhoet, R. (2013). Country-wide rainfall maps from cellular communication networks. *Proceedings of the National Academy of Sciences*, *110*(8), 2741–2745. https://doi.org/10.1073/pnas.1217961110

Overeem, A., Leijnse, H., & Uijlenhoet, R. (2016a). Retrieval algorithm for rainfall mapping from microwave links in a cellular communication network. *Atmospheric Measurement Techniques*, *9*(5), 2425–2444. https://doi.org/10.5194/amt-9-2425-2016

Overeem, A., Leijnse, H., & Uijlenhoet, R. (2016b). Two and a half years of country-wide rainfall maps using radio links from commercial cellular telecommunication networks: Two and a half years of radio link rainfall maps. *Water Resources Research*, *52*, 8039–8065. https://doi.org/10.1002/2016WR019412

Rahimi, A. R., Holt, A. R., Upton, G. J. G., & Cummings, R. J. (2003). Use of dual-frequency microwave links for measuring path-averaged rainfall. *Journal of Geophysical Research (Atmospheres)*, *108o*, 4467.

Rieckermann, J., Lüscher, R., & Krämer, S. (2009). Assessing urban precipitation using radio signals from a commercial communication network. In *8th International Workshop on Precipitation in Urban Areas*, St. Moritz, Switzerland (pp. 10–13).

Rincon, R. F., & Lang, R. H. (2002). Microwave link dual-wavelength measurements of path- average attenuation for the estimation of drop size distributions and rainfall. *IEEE Transactions on Geoscience and Remote Sensing*, *40*(4), 760–770.

Rios Gaona, M. F., Overeem, A., Brasjen, A. M., Meirink, J. F., Leijnse, H., & Uijlenhoet, R. (2017). Evaluation of rainfall products derived from satellites and microwave links for The Netherlands. *IEEE Transactions on Geoscience and Remote Sensing*, *55*(12), 6849–6859. https://doi.org/10.1109/TGRS.2017.2735439

Rios Gaona, M. F., Overeem, A., Leijnse, H., & Uijlenhoet, R. (2015). Measurement and interpolation uncertainties in rainfall maps from cellular communication networks. *Hydrology and Earth System Sciences*, *19*(8), 3571–3584. https://doi.org/10.5194/hess-19-3571-2015

Rios Gaona, M. F., Overeem, A., Raupach, T. H., Leijnse, H., & Uijlenhoet, R. (2018). Rainfall retrieval with commercial microwave links in Sao Paulo, Brazil. *Atmospheric Measurement Techniques*, *11*(7), 4465–4476.

Robertson, S., & King, A. (1946). The effect of rain upon the propagation of waves in the 1- and 3-centimeter regions. *Proceedings of the IRE*, *34*(4), 178p–180p. https://doi.org/10.1109/JRPROC.1946.234239

Roy, V., Gishkori, S., & Leus, G. (2016). Dynamic rainfall monitoring using microwave links. *EURASIP Journal on Advances in Signal Processing*, *2016*(1), 77.

Ruf, C. S., Aydin, K., Mathur, S., & Bobak, J. P. (1996). 35-GHz dual-polarization propagation link for rain-rate estimation. *Journal of Atmospheric and Oceanic Technology*, *13*(2), 419–425.

Scheidegger, A., & Rieckermann, J. (2014). Bayesian assimilation of rainfall sensors with fundamentally different integration characteristics. In *WRaH Proceedings*. Washington, DC: International Weather Radar and Hydrology symposium.

Schip, T. I. V. H., Overeem, A., Leijnse, H., Uijlenhoet, R., Meirink, J. F., & Delden, A. J. V. (2017). Rainfall measurement using cell phone links: classification of wet and dry periods using geostationary satellites. *Hydrological Sciences Journal*, *62*(9), 1343–1353. https://doi.org/10.1080/02626667.2017.1329588

Schleiss, M., & Berne, A. (2010). Identification of dry and rainy periods using telecommunication microwave links. *Geoscience and Remote Sensing Letters, IEEE*, *7*(3), 611–615. https://doi.org/10.1109/LGRS.2010.2043052

Schleiss, M., Rieckermann, J., & Berne, A. (2013). Quantification and modeling of wet- antenna attenuation for commercial microwave links. *IEEE Geoscience and Remote Sensing Letters*, *10*(5), 1195–1199. https://doi.org/10.1109/LGRS.2012.2236074

Swedish Meteorological and Hydrological Institute (2015). *Micro weather*. Sweden: Swedish Meteorological and Hydrological Institute. Retrieved from https://www.smhi.se/en/services/professional-services/micro-weather-live-data/

Smiatek, G., Keis, F., Chwala, C., Fersch, B., & Kunstmann, H. (2017). Potential of commercial microwave link network derived rainfall for river runoff simulations. *Environmental Research Letters.*, *12*, 034026. https://doi.org/10.1088/1748-9326/aa5f46

Sohail Afzal, M., Shah, S. H. H., Cheema, M. J. M., & Ahmad, R. (2018). Real time rainfall estimation using microwave signals of cellular communication networks: a case study of Faisalabad, Pakistan. *Hydrology and Earth System Sciences Discussions*, *2018*, 1–20. https://doi.org/10.5194/hess-2017-740

Stratton, J. (1930). The effect of rain and fog on the propagation of very short radio waves. *Proceedings of the Institute of Radio Engineers*, *18*(6), 1064–1074. https://doi.org/10.1109/JRPROC.1930.222101

Trömel, S., Ziegert, M., Ryzhkov, A. V., Chwala, C., & Simmer, C. (2014). Using microwave backhaul links to optimize the performance of algorithms for rainfall estimation and attenuation correction. *Journal of Atmospheric and Oceanic Technology*, *31*(8), 1748–1760. https://doi.org/10.1175/JTECH-D-14-00016.1

Uijlenhoet, R., Overeem, A., & Leijnse, H. (2018, July). Opportunistic remote sensing of rainfall using microwave links from cellular communication networks. *Wiley Interdisciplinary Reviews: Water*, *5*(4), e1289. https://doi.org/10.1002/wat2.1289

Ulbrich, C. W., & Lee, L. G. (1999). Rainfall measurement error by wsr-88d radars due to variations in z-r law parameters and the radar constant. *Journal of Atmospheric and Oceanic Technology*, *16*(8), 1017–1024. https://doi.org/10.1175/1520-0426(1999)016<1017:RMEBWR>2.0.CO;2

Upton, G., Cummings, R., & Holt, A. (2007). Identification of melting snow using data from dual-frequency microwave links. *Microwaves, Antennas & Propagation, IET*, *1*(2), 282–288. https://doi.org/10.1049/iet-map:20050285

van Leth, T. C., Overeem, A., Leijnse, H., & Uijlenhoet, R. (2018, August). A measurement campaign to assess sources of error in microwave link rainfall estimation. *Atmospheric Measurement Techniques*, *11*(8), 4645–4669. https://doi.org/10.5194/amt-11-4645-2018

Vörösmarty, C. J., Green, P., Salisbury, J., & Lammers, R. B. (2000). Global water resources: Vulnerability from climate change and population growth. *Science*, *289*(5477), 284–288. https://doi.org/10.1126/science.289.5477.284

Wang, Z., Schleiss, M., Jaffrain, J., Berne, A., & Rieckermann, J. (2012). Using Markov switching models to infer dry and rainy periods from telecommunication microwave link signals. *Atmospheric Measurement Techniques*, *5*(7), 1847–1859. https://doi.org/10.5194/amt-5-1847–2012

Zinevich, A., Alpert, P., & Messer, H. (2008). Estimation of rainfall fields using commercial microwave communication networks of variable density. *Advances in Water Resources*, *31*(11), 1470–1480. https://doi.org/10.1016/j.advwatres.2008.03.003

Zinevich, A., Messer, H., & Alpert, P. (2010). Prediction of rainfall intensity measurement errors using commercial microwave communication links. *Atmospheric Measurement Techniques*, *3*, 1385–1402.

How to cite this article: Chwala C, Kunstmann H. Commercial microwave link networks for rainfall observation: Assessment of the current status and future challenges. *WIREs Water*. 2019;6:e1337. https://doi.org/10.1002/wat2.1337